

# A molecular dynamics study on bubble growth in tungsten under helium irradiation

Ryo KOBAYASHI,<sup>1,\*</sup> Tatsunori HATTORI,<sup>1</sup> Tomoyuki TAMURA,<sup>2</sup> and Shuji OGATA<sup>1</sup>

*<sup>1</sup>Department of Scientific and Engineering Simulation,  
Nagoya Institute of Technology, Gokiso-cho,  
Showa-ku, Nagoya 466-8555, Japan*

*<sup>2</sup>Center for Fostering Young and Innovative Researchers,  
Nagoya Institute of Technology, Gokiso-cho,  
Showa-ku, Nagoya 466-8555, Japan*

## Abstract

Molecular dynamics simulation has been performed to investigate the effects of irradiated helium atoms in tungsten on the bubble nucleation and the dislocation loop formation. Simulation results clearly show that helium atoms in tungsten tend to migrate as isolated interstitials at high temperatures and to be absorbed to existing tungsten-vacancies or defects such as bubbles or dislocations. Tungsten self-interstitial atoms pushed out from the helium bubble tend to stay in the vicinity of the bubble and, then form a dislocation loop when the number of the atoms exceed the threshold. Since the bubbles and dislocation loops cause further nucleation of bubbles, there appears a helium bubble array along  $\langle 111 \rangle$  direction. The bubble growth rate within this self induced bubble growth mechanism will be much faster than than that of existing growth model. The growth model needs to be reformulated by taking the self-induced effects into account.

PACS numbers: 61.72.Ff, 61.72.Hh, 07.05.Tp, 61.43.Bn

Keywords: molecular dynamics, helium bubble growth, dislocation loop

---

\* kobayashi.ryo@nitech.ac.jp

## I. INTRODUCTION

Tungsten (W) is considered to be the most promising candidate as a plasma-facing material (PFM) at the divertor in nuclear fusion plants due to its excellent properties such as high melting temperature, high thermal conductivity, and low sputtering rate. Since the PFM is exposed to high energy helium (He), deuterium (D), tritium (T) ions, and neutrons, a lot of research about irradiation effects on W surface has been done so far. It is known that bubbles and dislocation loops, which are main causes of the degradation of mechanical properties of the material, are formed depending on the temperature of the material, fluence, and incident energy of He irradiation. For example, bubble size is highly dependent on the temperature; the higher the temperature, the larger the bubbles become.[1]

Not only the defects deep inside the material, a surface nanostructure induced by the He irradiation was found by Takamura *et al.*[2] Interestingly the nanostructure can be formed under He irradiation with very low incident energy less than 50 eV and without any irradiation such as deuterium and tritium ions. The surface nanostructure, so called fuzz structure, has some interesting features such as large surface area and almost perfect absorption of incident light, which attract many researchers in other fields for applying the structure to other devices like catalysts, solar cells, or electron emitters.[3–7] Since there are always He bubbles and dislocation loops as precursors of the fuzz structure, to avoid the formation or to control the character of the fuzz structure, we have to understand how bubbles and dislocation loops grow under He irradiation condition.

A lot of theoretical studies using computer simulation approaches such as *ab initio*,[8–14] molecular dynamics (MD),[15–19] and kinetic Monte Carlo (KMC)[20] have been performed to investigate He migration, He clustering, bubble formation, and dislocation loop punching. There are also some theoretical model based on the rate theory which takes into account the reactions observed in the studies mentioned above.[21] However still we don't have the theoretical model that predicts quantitatively the nucleation and growth rates of He bubbles. Thus the purpose of this paper is to study the fundamental mechanism of the initial stage of bubble growth in the case that only He atoms exist in W crystal, because the bubbles and dislocation loops are observed under irradiation of only He ions with very low incident energy.

In this paper, we perform large scale MD simulation to make clear the He bubble nucleation and growth mechanism in bulk W under the condition that many He atoms exist having lost their energies after the He irradiation and migrating on interstitial sites. Section II describes the details of computation method. In Sec. III B, a rough estimate of the temperature dependence of bubble size in the ideal situation is discussed, and the MD simulation results of novel bubble growth mechanism is shown in Sec. III A. And we conclude the present work in Sec. IV.

## II. COMPUTATION METHOD

We adopt  $NVT$ -ensemble MD simulation [22] to investigate the behavior of He atoms and its effects on the defect formation in W bulk. In the MD simulation, time integration is performed using the velocity-Verlet method and time interval is chosen to 1 fs. We adopt the Berendsen thermostat method[23] for controlling the temperature. The temperature of He atoms are also controlled by the thermostat even after bubbles are nucleated. We have also performed  $NVE$  simulation after the equilibration and confirmed the results don't change qualitatively.

For the interatomic potential of W-W, W-He, and He-He, we adopt Ito potential[19] which is based on Finnis-Sinclair potential modified by Ackland and Thetford.[24, 25] Bulk properties of W and properties related to He interstitials obtained by the present potential are listed in Table I. The bulk properties are worse than those obtained by Li potential[26], however He interstitial properties and migration barrier of He agree well with *ab initio* values. In addition, the cutoff radius of the Ito potential is rather shorter than the other existing interatomic potentials and Ito potential does not have an angular term which usually costs much. Hence the MD simulation with the Ito potential runs very fast, which is practically important when we perform large-scale and long-time simulation; for example, the computational cost of Ito potential is about 1/40 of that of Li potential.

All the MD simulation runs are performed using our own program, NAP (Nagoya Atomistic-simulation Package)[28], which enables us to perform massively parallel MD simulation with spatial decomposition technique. The simulation system is a cubic periodic supercell of bcc crystalline W including He atoms that are randomly placed at tetrahedron

TABLE I. Comparison of physical properties obtained using the Ito potential. W bulk properties such as lattice constant  $a$ , bulk modulus  $B$ , vacancy formation energy  $E_{\text{vac}}$ , formation energy of self interstitial  $E_{\text{SIA}}$ , and W-He properties such as the formation energies of He interstitials at tetrahedral site  $E_{\text{tetra}}$ , octahedral site  $E_{\text{octa}}$ , trigonal site  $E_{\text{tri}}$ , and migration barrier  $E_{\text{mig}}$  are listed.

	Ito pot.	Li pot.[26]	<i>ab initio</i>
$a$ (Å)	3.204	3.165	3.17[9]
$B$ (GPa)	306	306	314[27]
$E_{\text{vac}}$ (eV)	4.33	3.54	3.11[10]
$E_{\text{SIA}}$ (eV)	11.11	9.74	9.4-11.6[11]
$E_{\text{tetra}}$ (eV)	6.58	6.23	6.16[9]
$E_{\text{octa}}$ (eV)	6.82	7.49	6.38[9]
$E_{\text{tri}}$ (eV)	6.65	6.25	6.35[14]
$E_{\text{mig}}$ (eV)	0.07	0.02	0.06[9, 14]

sites at the beginning of the simulation. Random distribution of He atoms is a reasonable assumption, because it is considered that He ions lose their ionization energies at the W surface and their incident energies through collisions with W atoms, as a result He atoms thermally migrate in W crystal.[29] Numbers of W atoms and He atoms are 2 million and about 10,000, respectively, and the edge length of the cell is about 32 nm. This He density corresponds to the fluence of about  $10^{20} \text{ m}^{-2}$  under the assumption that none of injected He atoms leaves the system, which is unlikely in the real situation and usually He atoms get out of the material by migrating and reaching to the surface. **Thus one cannot compare the fluence value directly to that of experiments and the density would be much higher than the real situation, however it is expected that simulation results involve the underlying physics of bubble nucleation.** The system size is determined through preliminary  $NpT$  simulation with a small system cell and fixed during the simulation runs. Although we have confirmed that the insertion of He atoms of such density does not affect the internal pressure through the test simulation with a small cell, the pressure in the system may change during the simulation after nucleating He bubbles and dislocation loops. We perform several cases in

temperature from 500 K up to 2000 K. In all the cases we put a single vacancy in the system in order to enhance bubble nucleation. It is not necessary because in all the cases vacancies are nucleated when we wait long enough.

Defects, distorted structures, and He atoms are extracted using the common neighbor analysis (CNA) technique.[30] In order to detect bcc structures, the cutoff radius in the CNA is set to longer than the second nearest and shorter than the third nearest atomic distances. The CNA enables us to eliminate the atoms that stay at regular bcc positions from the visualization and to see self-interstitial atoms (SIAs) and dislocations, as shown in Figs. 1 and 2.

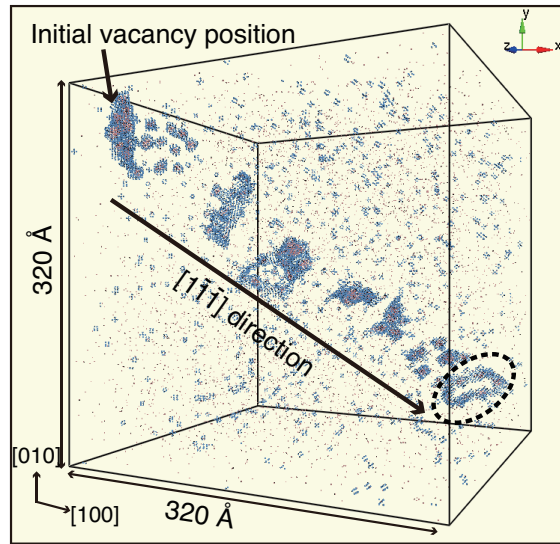


FIG. 1. The cell used in this simulation runs. Atomic configuration at 2000 K after 6 ns from the random distribution of He atoms is also shown. Only displaced W atoms and He atoms are shown. The leading dislocation loop is indicated by a broken circle.

### III. RESULTS AND DISCUSSION

#### A. Self-induced bubble growth

We find successive bubble nucleations and growth, which we call *self-induced bubble growth*, through visual inspection of the MD simulation at 2000 K. Once an embryonic

bubble is nucleated, the bubble grows rapidly by absorbing migrating He interstitials and pushing out the W atoms surrounding the bubble. The W atoms pushed out from the bubble do not go away from the bubble as isolated SIAs but stay around the bubble like a cloud covering the bubble as shown in Fig. 2(a). This is slightly different from the MD work by Zhou *et al.*,[13] but consistent with previous molecular dynamics/statics studies.[15, 16] Considering the high formation energy of W SIA (see Table I), single SIA going away from the bubble seems unlikely and thus creating the SIA cloud around the bubble is reasonable.

The SIA cloud makes the deformation field around the bubble; the place of the cloud itself is compressive and the outside of the cloud becomes tensile. The tensile field attracts He interstitials and enhances the nucleation of further bubble as shown in Fig. 2(b). The SIAs are emitted as a dislocation loop along  $\langle 111 \rangle$  (Fig. 2(c)), when the bubble grows and the SIA cloud exceeds the threshold size, which is very small and the smallest dislocation loop observed is less than 10 Å in diameter. The dislocation loop, which is made of edge dislocation having  $\langle 111 \rangle a/2$  Burgers vector where  $a$  is the lattice constant, also attracts He interstitials and enhances further bubble nucleation (indicated by arrows in Fig. 2(d)). As a consequence, once a bubble is nucleated, a bubble array will be formed along  $\langle 111 \rangle$  within a very short period as illustrated in Fig. 1. The bubbles nucleated close to each other are likely to merge into one bigger bubble, as shown in Fig. 2(d), when they grow and the separation between them becomes thin enough to be broken by the pressure of He bubbles. Therefore the growth and nucleation rates of bubbles seem to be much larger than those of the case without this self-induced mechanism.

Dislocation loops can be emitted to any  $\langle 111 \rangle$  directions, as shown in Fig. 1 (inside the broken circle). Since it is unlikely for a dislocation loop to change its direction due to the energetic reason, dislocation loops tend to keep moving on a certain  $\langle 111 \rangle$  direction. We can expect that, once a dislocation loop is nucleated on different  $\langle 111 \rangle$  line, the loop runs on the line and the trail made of embryonic He bubbles appears on the line. As a consequence, the network made of small bubbles lying on  $\langle 111 \rangle$  lines can be formed.

We have to notice that the shape of bubbles nucleated and grown in this self-induced mechanism will not be kept elongated in  $\langle 111 \rangle$  direction in the long run such as a period of 1 sec or longer which is a common time scale in most experiments.[1, 31] Even if the bubbles nucleated along  $\langle 111 \rangle$  coalesce into large and elongated bubble, W atoms at the surface of

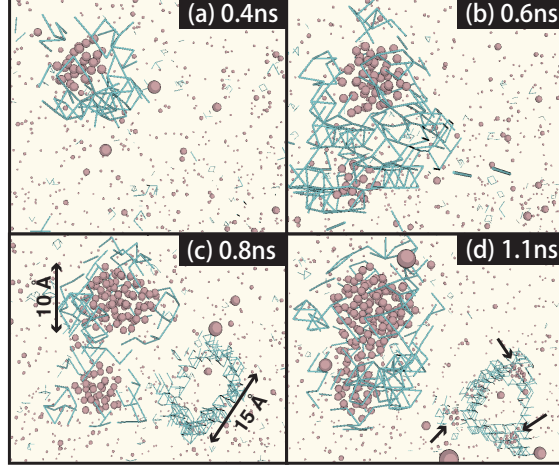


FIG. 2. Snapshots of an MD simulation run at 2000 K. Only He atoms (purple circles) and W-W bonds (green lines) distorted from bcc ones are shown. Interstitial W atoms pushed out from a bubble stay around the bubble making distorted W-W bonds up to 0.6 ns. A dislocation loop is emitted from the bubble at 0.8 ns. Arrows in (d) indicate new embryonic bubbles nucleated at the edge of the dislocation loop.

the bubble can migrate during a long period of time and the bubble tends to become stable faceted shape from the view point of the free energy. Therefore it is not easy to observe the arrays of small bubbles in the experiments.

### B. Temperature dependence of cluster-size population

Figure 3 shows He cluster (and bubble) population as a function of the number of He atoms in a cluster at 500, 1000, and 2000 K, after 2 ns from the initial configuration in which He atoms are randomly distributed at tetrahedral sites. We define the He cluster as a group of He atoms in which any He atom has at least one close neighboring He atom within 2 Å. These graphs clearly show that there appear a lot of clusters including less than 20 atoms at 500 K (Fig. 3(a)), on the other hand, at 2000 K, there are some large clusters including over 20 atoms which we call bubbles, fewer small clusters, and a lot of single He atoms (Fig. 3(c)). From the MD results, we can see that He bubbles are formed when the temperature is high enough for He atoms to be able to escape from small He clusters and

reach larger bubbles.

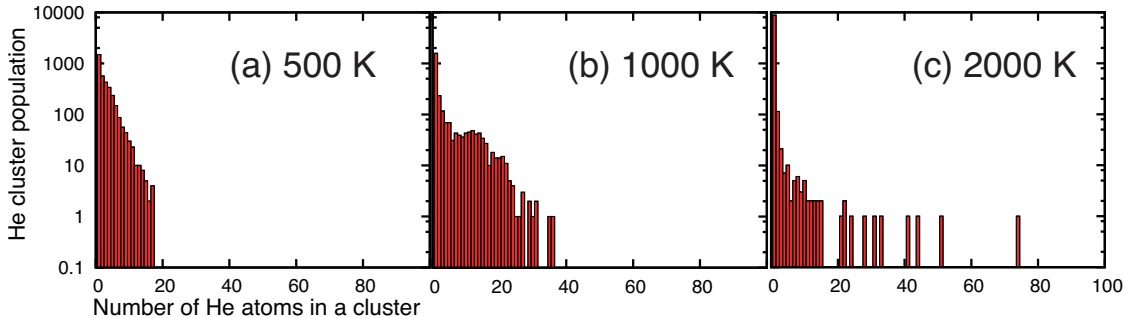


FIG. 3. He cluster population as a function of the cluster size after 2 ns from random distribution of He atoms. There are a lot of small clusters in case of 500 K, whereas there are some large clusters at 2000 K.

We can understand this temperature dependency of He cluster population by considering the free energy of creation of He clusters. It is known that He atoms in W crystal attract each other and have high binding energy from the *ab initio* study by Becquart and Domain.[9] However, entropic contribution cannot be ignored when we think whether or not He atoms gather and create clusters at rather high temperature. We assume the total number of He atoms,  $n$ , in the system is constant and there are  $n_m$  clusters which include  $m$  He atoms in each of them,

$$\sum_{m=1}^M mn_m = n_1 + 2n_2 + \dots + Mn_M = n, \quad (1)$$

where  $M$  is the maximum number of He atoms in a cluster. The total free energy,  $F$ , and the free energy of He clusters including  $m$  He atoms,  $F_m$ , are defined as follows,

$$\begin{aligned} F &= \sum_m^M F_m, \\ F_m &= n_m E_m - k_B T \ln_N C_{n_m} \\ &\simeq n_m E_m - k_B T \{ N \ln N - (N - n_m) \ln(N - n_m) \\ &\quad - n_m \ln n_m \}, \end{aligned} \quad (2)$$

where  $E_m$ ,  $k_B$ ,  $T$ , and  $N$  are the binding energy of  $m$ -He cluster, Boltzmann factor, temperature, and number of He sites in bcc W crystal, which is much larger than the number



of He atoms, that is  $1 \ll n \ll N$ , respectively. Computing the set of  $\{n_m\}$  which minimizes the total free energy with respect to the given temperature, we obtain the population of He clusters as a function of temperature. The binding energies,  $\{E_m\}$ , obtained through the molecular statics calculation using Ito potential with a small simulation cell including 250 W atoms and edge length being 16 Å are  $(E_1, E_2, E_3, E_4, E_5) = (0.00\text{eV}, -0.25\text{eV}, -0.69\text{eV}, -1.21\text{eV}, -2.01\text{eV})$ , where we assume  $M = 5$  here.

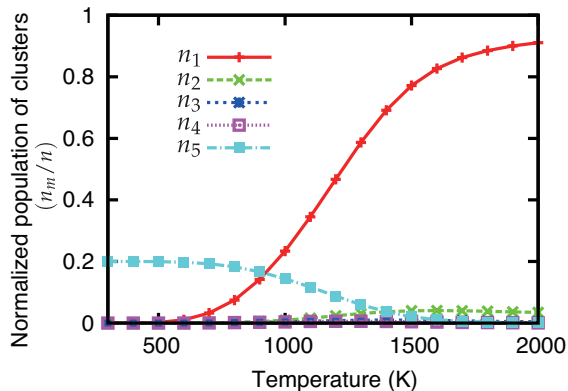


FIG. 4. Normalized population of He clusters,  $n_m/n$ , as a function of temperature.

Figure 4 shows the calculated population of He clusters as a function of temperature. At the low temperature, He atoms tend to gather and create small clusters, 5-member cluster ( $\text{He}_5$ ) in this case. At the high temperature above 1000 K, single He atom ( $\text{He}_1$ ) is the major form, however there are still considerable amount of  $\text{He}_5$  clusters up to about 1500 K. These results are partly consistent with the results of the MD simulation as shown in Fig. 3; both results show high population of single He atoms at high temperatures and small but larger than 5-member clusters at low temperatures. However, in the case of high temperature, there exists a significant difference between this analysis and the MD result; there are some large clusters in the MD simulation. This is because the nucleation of He bubbles, dislocation loops, and self-induced bubble nucleation is not taken into account in the free-energy analysis.

## IV. CONCLUSION

We have performed the large-scale MD simulation of W crystal including He atoms at random tetrahedron sites to investigate the nucleation and growth of defects such as a He bubble and a dislocation loop. We have found the self-induced bubble growth mechanism and that there appear the arrays of small bubbles along  $\langle 111 \rangle$  direction in a short period of time. The theoretical model of the He-bubble growth such as the KMC and the model based on the rate theory should be reformulated to take into account the self-induced growth mechanism to correctly describe the growth rate of the bubble in a bulk W crystal. Note that, in the paper, we only focus on He atoms in W, but D and T ions also exist in real fusion reactors. Since the binding energy of He atom to vacancy is much higher than D/T to vacancy,[32, 33] we can expect that the results obtained here do not change significantly. However it is highly possible that the existence of D/T changes the rate of bubble growth and dislocation migration speed, thus the simulation including He and D/T needs to be conducted in the future study.

## ACKNOWLEDGMENTS

Authors thank Dr. A. Ito for motivating us to do this work and providing us the interatomic potential he made. This research was supported by NIMS Program for Cross-disciplinary Study, JSPS KAKENHI Grant-in-Aid for Young Scientists B 24740201, and IFERC-CSC.

- 
- [1] H. Iwakiri, K. Yasunaga, K. Morishita, and N. Yoshida, *Journal of Nuclear Materials* **283-287**, 1134 (2000).
  - [2] S. Takamura, N. Ohno, D. Nishijima, and S. Kajita, *Plasma and Fusion Research* **1**, 051 (2006).
  - [3] M. Baldwin and R. Doerner, *Nuclear Fusion* **48**, 035001 (2008).
  - [4] S. Kajita, W. Sakaguchi, N. Ohno, N. Yoshida, and T. Saeki, *Nuclear Fusion* **49**, 095005 (2009).

- [5] S. I. Krasheninnikov, *Physica Scripta* **T145**, 014040 (2011).
- [6] S. Kajita, T. Yoshida, D. Kitaoka, R. Etoh, M. Yajima, N. Ohno, H. Yoshida, N. Yoshida, and Y. Terao, *Journal of Applied Physics* **113**, 134301 (2013).
- [7] S. Takamura, *Plasma and Fusion Research* **9**, 1302007 (2014).
- [8] P. Derlet, D. Nguyen-Manh, and S. Dudarev, *Physical Review B* **76**, 054107 (2007).
- [9] C. Becquart and C. Domain, *Physical Review Letters* **97**, 196402 (2006).
- [10] C. S. Becquart and C. Domain, *Nuclear Instruments and Methods in Physics Research B* **255**, 23 (2007).
- [11] L. Chen, Y. Liu, H. Zhou, S. Jin, Y. Zhang, and G.-H. Lu, *Science China Physics, Mechanics and Astronomy* **55**, 614 (2012).
- [12] L. Ventelon, F. Willaime, C.-C. Fu, M. Heran, and I. Ginoux, *Journal of Nuclear Materials* **425**, 16 (2012).
- [13] Y. Zhou, J. Wang, Q. Hou, and A. Deng, *Journal of Nuclear Materials* **446**, 49 (2014).
- [14] T. Tamura, R. Kobayashi, S. Ogata, and A. M. Ito, *Modelling and Simulation in Materials Science and Engineering* **22**, 015002 (2014).
- [15] W. D. Wilson, C. L. Bisson, and M. I. Baskes, *Physical Review B* **24**, 5616 (1981).
- [16] K. Morishita, B. D. Wirth, T. D. D. Rubia, and A. Kimura, *Effects of Helium on Radiation Damage Processes in Iron*, Tech. Rep. (2001).
- [17] K. Henriksson, K. Nordlund, and J. Keinonen, *Nuclear Instruments and Methods in Physics Research Section B: Beam Interactions with Materials and Atoms* **244**, 377 (2006).
- [18] F. Sefta, N. Juslin, and B. D. Wirth, *Journal of Applied Physics* **114**, 243518 (2013).
- [19] A. M. Ito, Y. Yoshimoto, S. Saito, A. Takayama, and H. Nakamura, *Physica Scripta* **T159**, 014062 (2014).
- [20] Q. Hou, Y. Zhou, J. Wang, and A. Deng, *Journal of Applied Physics* **107**, 084901 (2010).
- [21] Y. Li, W. Zhou, L. Huang, Z. Zeng, and X. Ju, *Journal of Nuclear Materials* **431**, 26 (2012).
- [22]  $NVE$ ,  $NVT$ , and  $NpT$  are abbreviations of physical parameters to be conserved during the simulation; for example,  $NpT$  for constant number of atoms, constant pressure, and constant temperature.
- [23] C. Berendsen, P. M. Postma, W. F. V. Gunsteren, A. Dinola, and R. Haak, *Journal of Chemical Physics* **81**, 3684 (1984).

- [24] M. W. Finnis and J. E. Sinclair, *Philosophical Magazine A* **50**, 45 (1984).
- [25] G. J. Ackland and R. Thetford, *Philosophical Magazine A* **56**, 15 (1987).
- [26] X.-C. Li, X. Shu, Y.-N. Liu, Y. Yu, F. Gao, and G.-H. Lu, *Journal of Nuclear Materials* **426**, 31 (2012).
- [27] F. H. Featherston and J. R. Neighbours, *Physical Review* **130**, 1324 (1963).
- [28] <https://github.com/ryokbys/nap>.
- [29] S. Saito, A. Takayama, A. M. Ito, and H. Nakamura, *Journal of Nuclear Materials* **438**, S895 (2013).
- [30] J. D. Honeycutt and H. C. Andersen, *Journal of Physical Chemistry* **91**, 4950 (1987).
- [31] K. Ono, M. Miyamoto, K. Arakawa, and R. Birtcher, *Philosophical Magazine* **89**, 513 (2009).
- [32] H.-B. Zhou, Y.-L. Liu, S. Jin, Y. Zhang, G.-N. Luo, and G.-H. Lu, *Nuclear Fusion* **50**, 115010 (2010).
- [33] G.-H. Lu, H.-B. Zhou, and C. S. Becquart, *Nuclear Fusion* **54**, 086001 (2014).